Locating Multiple Camera Sensors and Wireless Access Points for a Generalized Indoor Positioning System

Jaime Duque Domingo,
Carlos Cerrada
and J.A. Cerrada

Departamento de Ingeniería de Software y
Sistemas Informáticos
ETSI Informática, UNED,
C/Juan del Rosal, 16. 28040 Madrid, Spain
Email: `ccerrada@issi.uned.es`

Enrique Valero

School of Energy, Geoscience, Infrastructure and Society,
Heriot-Watt University,
Edinburgh EH14 4AS, United Kingdom
Email: `e.valero@hw.ac.uk`

Abstract—This work illustrates the generalization of a previously developed Indoor Positioning System (IPS) based on the combination of WiFi Positioning System (WPS) and depth maps. This generalization extends the use of the proposed system to scenarios containing multiple rooms and several people, in contrast to the more simpler initial version. The combination of both technologies improves the efficiency of existing methods, based uniquely on wireless positioning techniques, for estimating the location of people. Users just require the use of smart-phones, besides the installation of RGB-D devices in the sensing area. But some problems arise when multiple RGB-D sensors and access points must be located in a large area composed of several rooms. The paper exposes how the necessary devices are placed minimizing the total uncovered area. Experimental results for an office space composed by nine differently sized rooms are shown.

Keywords–indoor positioning; IPS; WPS; RGB-D sensors; Kinect; WiFi; fingerprint; trajectory; skeletons; depth map.

I. Introduction

Indoor Positioning Systems (IPSs) are used to obtain the position of people or objects inside a building [1]. This work extends a previously developed method for indoor positioning inside a room [2], in which WiFi Positioning System (WPS) and RGB-D sensors are combined. Object recognition can be considered as a part of the core research area of computer vision, and an important number of authors have reported methods and applications for people detection and positioning. The generalization of the previous IPS will deliver the position of users in complete scenarios where there are several people interacting with the environment. Trajectories of users will be obtained by means of the two considered information sources: WPS values and trajectories of the skeletons of users in the *depth map*. While location of wireless sensors does not represent any real problem, special care must be taken in the location of the depth cameras in order to minimize the total uncovered area. In fact, several Kinect v2 sensors should be used simultaneously during experiments to capture the skeletons of users evolving through different rooms. This work shows how coordinates obtained by these sensors placed in different rooms are transformed into a Universal Coordinates System (UCS).

The paper is structured as follows: Section II explores existing solutions concerning positioning, based on WPS, RGB-D sensors, and using both technologies in a joint manner. Section III is devoted to analyze the proposed system and compare it to the previous one. Special attention is given to describe how the multiple cameras should be located in a large area as considered, and how their respective coordinate systems should be related to the universal coordinate system. Section IV presents the layout in which the experiments were performed and analyzes the main obtained results. Finally, Section V states the conclusions of the work.

II. Overview of related work

WPS is founded on the *fingerprinting* technique [3]. This technique creates a map of the environment recording the *Received Signal Strength Indication* (RSSI) in each point. RSSI is a reference scale used to measure the power level of signals received from a device on a wireless network (usually WiFi or mobile telephony). This map is used to obtain the position of a user in real-time, comparing the values received from the user's portable device to those stored in the map. A recent comparison between WiFi fingerprint-based indoor positioning systems have been presented in [4]. Regarding the use of advanced techniques, authors explain how to make use of temporal or spatial signal patterns, user collaboration, and motion sensors. Also, authors discuss recent advances on reducing offline labor-intensive survey, adapting to fingerprint changes, calibrating heterogeneous devices for signal collection, and achieving energy efficiency for smartphones.

In the field of people and objects detection, other technologies based on computer vision (e.g., RGB-D sensors) have been increasingly used. Authors, in [5], developed a method to detect and identify several people that are occluded by others in a scene. In [6], authors propose a *smart-cane* for the visually impaired that, with the help of a Kinect sensor, facilitates the location of objects. And the method *Kinect Positioning System* (KPS) is analyzed in [7] aiming to obtain the user position. These positioning techniques have also been used in Robotics, such as the work presented in [8], where several *Simultaneous Localization and Mapping* (SLAM) algorithms are proposed for building maps with robots. By means of

SLAM, the environment is built recording the measurements RSSI in each point. Also, in this field of research, the use of different technologies improves positioning systems as shown in [9], where authors analyze how to generate a *fingerprint map* with an RGB-D sensor mounted on a robot.

The work in [10] proposes a hybrid indoor positioning system where WiFi and *Global System for Mobile communication* (GSM) are combined for indoor positioning. Three positioning algorithms from the Nearest Neighbor (NN) family are used for simulations. An architecture for improving indoor positioning, by means of the combination of WiFi and RFID, is presented in [11]. WiFi is used for coordinating the RFID readers when accessing the channel for retrieving tag identifications. This avoids, in the presence of multiple readers, the so-called reader collision problem that RFID suffers from. This problem is caused by the inability for direct communication among them. In [12], a robot is located by using three different systems: a laser rangefinder, a depth camera, and RSSI values. Each system is independently used according to the zone where the robot is located.

The present work extends a previously developed method for indoor positioning inside a room [2], which considers a scenario as represented in Figure 1. That work combined two known technologies: WPS, widely used for indoor positioning, and computer vision by means of RGB-D sensors. However, experiments were carried out just in a room, where the system was set up.
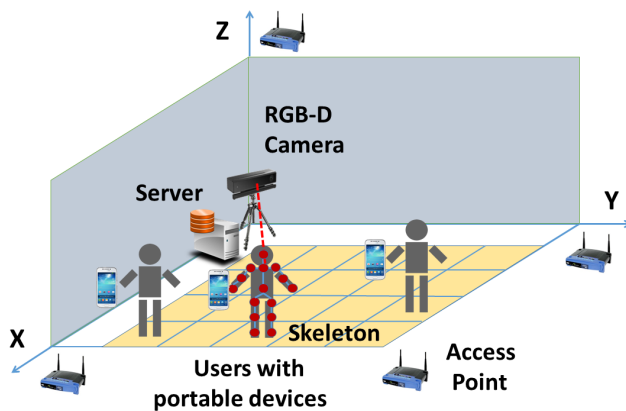

Figure 1. Scenario of the previous work

III. ANALYSIS OF THE GENERALIZED SYSTEM

The generalization of the previous IPS will deliver users identification and position in more complex scenarios (i.e. with more rooms) where several users are navigating. This system can be set up in departments or companies where monitoring the position of employees becomes useful to improve the efficiency of business. The trajectories of users will be calculated by combining the two mentioned information sources: WPS data and trajectories of the skeletons of users from the *depth map*. Skeletons are obtained by means of the techniques presented in [13] and [14], where authors propose new algorithms to quickly and accurately predict 3D positions of body joints from depth images. Those methods form a core component of the Kinect gaming platform.

As previously mentioned, the proposed system has been conceived to work in a scenario composed of various rooms (see Figure 2) where there are several people, each of them using a smartphone. Two or more RGB-D sensors are situated in each room to obtain the coordinates of users by means of their skeletons. From these skeletons, neck coordinates are extracted aiming to position people in the environment. This part of the body is chosen because it is less prone to be occluded by elements in the scenario.
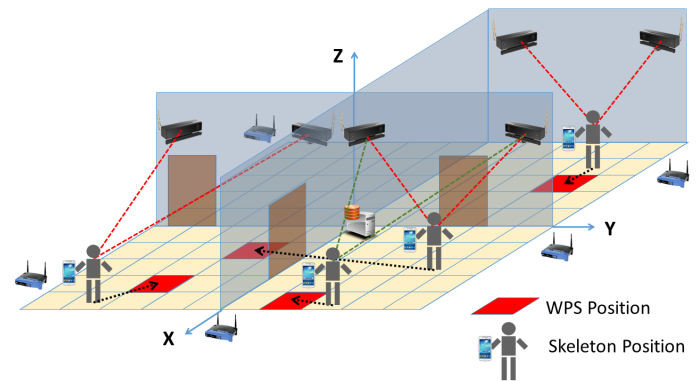

Figure 2. Scenario of the generalized system

The coordinates of the obtained skeletons are considered as illustrated in Figure 3. The distance from the sensor to the skeletons is measured along the Z_{RGB-D} axis, while Y_{RGB-D} axis represents the heights of the users.
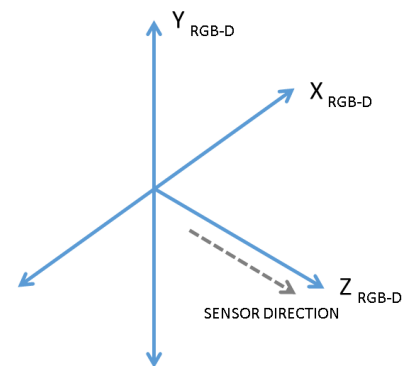

Figure 3. X_{RGB-D}, Y_{RGB-D}, and Z_{RGB-D} axis regarding the RGB-D sensor direction

As one unique Universal Coordinates System (UCS) is considered, the coordinates obtained by the RGB-D sensors are transformed to that this reference system. Only 2D coordinates are considered in this positioning system, as Y_{RGB-D} axis is ignored and Z_{RGB-D} axis corresponds to Y_{POS} axis by means of a transformation.

In order to transform the coordinates obtained by each camera into the UCS, it is necessary to use the angle of the camera and its distance to the universal center point $P(0,0)$.

Each RGB-D sensor has a different angle respect to the UCS and is situated at a different position.

In this work, Kinect sensors have been used as RGB-D sensors. They have a limited angle range (see Figure 4). For this reason, they are turned to obtain a 70° angle from the wall. This implies that it is necessary to calculate the coordinates they deliver into the UCS. These processes are described in the following subsections.

The use of more than one RGB-D sensor reduces the problem of uncovered areas. Since Kinect sensors obtain depth maps with a limited angle of 70°, the proposed system uses two or more Kinect sensors to detect users in all positions. In this manner, the parts which are not covered by a sensor are recorded by another one. In some cases, it is necessary to use more than two sensors because of the geometry of the scene. In addition, the system can discern if two RGB-D sensors are detecting the same user establishing a minimal distance between them. If one Kinect detects a user and this is located at 40cm of another user detected by another Kinect, then both users are considered the same.

A. Position of RGB-D sensors in a room

RGB-D sensors are placed drawing a maximum angle from the walls. As previously mentioned, in the case of Kinect v2, the sensor is able to obtain a 70° angle. To obtain the maximum coverage, the vision line must start at the opposite corner respect the sensor. The values of X_{POS} and Y_{POS} represent the position of the sensor (see Figure 4). Kinect v2 is 25 cm wide. L represents the length of the wall.
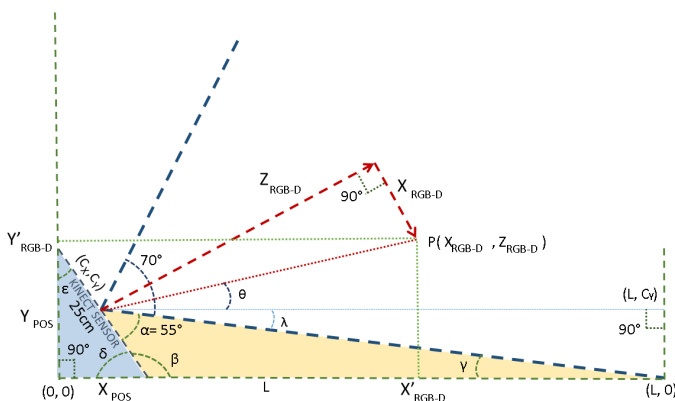

Figure 4. Position of the Kinect v2 sensor

Using the law of sines, it is possible to relate both triangles and obtain the value of X_{POS} with respect to L. The first triangle, the one described between the sensor and the wall, which is represented in light blue, is solved by (1).

$$\frac{25}{\sin 90°} = \frac{X_{POS}}{\sin \varepsilon} \quad (1)$$

where $90° + \varepsilon + \delta = 180°$. Therefore, (1) is simplified in (3).

$$\frac{25}{\sin 90°} = \frac{X_{POS}}{\sin(90° - \delta)} \quad (2)$$

$$X_{POS} = 25 \cdot \sin(90° - \delta) \quad (3)$$

The second triangle is the one formed between the sensor and the opposite corner, represented in light yellow (see Figure 4) and it is solved by (4).

$$\frac{L - X_{POS}}{\sin 55°} = \frac{12,5}{\sin \gamma} \quad (4)$$

where $55° + \beta + \gamma = 180°$ and $\beta + \delta = 180°$. Therefore, $\gamma = \delta - 55°$ and (4) can be modified as (6).

$$\frac{L - X_{POS}}{\sin 55°} = \frac{12,5}{\sin(\delta - 55°)} \quad (5)$$

$$X_{POS} = L - \frac{12,5 \cdot \sin 55°}{\sin(\delta - 55°)} \quad (6)$$

According to (3), it is possible to extract the value of δ (see (7)).

$$\delta = 90° - \arcsin\left[\frac{x}{25}\right] \quad (7)$$

Replacing δ in (6), X_{POS} is related to L (see (8)).

$$L = X_{POS} + \frac{12,5 \cdot \sin 55°}{\sin\left(35° - \arcsin\left[\frac{X_{POS}}{25}\right]\right)} \quad (8)$$

For example, if a Kinect v2 sensor is placed in a room with 430 cm wide ($L = 430$), X_{POS} will take the value $13,79$ using (8). Y_{POS} is obtained by Pythagoras' Theorem as seen in (9).

$$X_{POS}^2 + Y_{POS}^2 = 25^2 \quad (9)$$

Therefore, $Y_{POS} = 20,85$. So, the Kinect sensor has to be placed at $13,79cm$ from the corner where the 70° angle starts and at $20,85cm$ from the adjacent wall.

B. Position of RGB-D sensors respect to the UCS

The middle point of the Kinect sensor, (C_X, C_Y), has to be considered for the displacements in the UCS. This point is calculated using again the law of sines (see (10)).

$$\frac{25}{\sin 90} = \frac{X_{POS}}{\sin \varepsilon} = \frac{Y_{POS}}{\sin \delta} \quad (10)$$

$$\varepsilon = \arcsin\left(\frac{X_{POS}}{25}\right) \quad (11)$$

$$\delta = \arcsin\left(\frac{Y_{POS}}{25}\right) \quad (12)$$

$$\sin(\delta) = \frac{C_Y}{12,5} \quad (13)$$

$$\sin(\varepsilon) = \frac{C_X}{12,5} \tag{14}$$

Then, (15) is obtained and C_X and C_Y are calculated. Considering $x = 13,79cm$ and $y = 20,85cm$, then $C_X = 10,43$ and $C_Y = 6,90$.

$$\begin{cases} C_X = 12,5 \cdot \sin\left(\arcsin\left(\frac{Y_{POS}}{25}\right)\right) = \frac{Y_{POS}}{2} \\ C_Y = 12,5 \cdot \sin\left(\arcsin\left(\frac{X_{POS}}{25}\right)\right) = \frac{X_{POS}}{2} \end{cases} \tag{15}$$

Since the angle that creates the sensor with the wall is not straight, it is necessary to obtain the deviation λ. Again, this angle can be obtained using the law of sines by means of (16).

$$\frac{\sqrt{(L - C_X)^2 + (0 - C_Y)^2}}{\sin 90°} = \frac{C_Y}{\sin \lambda} \tag{16}$$

Simplifying (16), (17) is obtained, where λ takes the value $1,01°$ in the example.

$$\lambda = \arcsin \frac{C_Y}{\sqrt{(L - C_X)^2 + C_Y{}^2}} \tag{17}$$

Once λ is obtained, it is possible to obtain X'_{RGB-D} and Y'_{RGB-D}. These points represent the position of the skeleton with respect to the corner where the RGB-D sensor is located. The value d_{RGB-D} is obtained by (18). This is used to simplify the rest of expressions.

$$d_{RGB-D} = \sqrt{Z_{RGB-D}^2 + X_{RGB-D}^2} \tag{18}$$

Using the law of sines, the θ angle is calculated (see (19) and (20)).

$$\frac{d_{RGB-D}}{\sin 90} = \frac{X_{RGB-D}}{\sin(35 - \lambda - \theta)} \tag{19}$$

$$\theta = 35 - \lambda - \arcsin\left(\frac{X_{RGB-D}}{d_{RGB-D}}\right) \tag{20}$$

X'_{RGB-D} and Y'_{RGB-D} are obtained using the X_{RGB-D} and Z_{RGB-D} coordinates of the skeleton obtained by the sensor (see (21)).

$$\begin{cases} X'_{RGB-D} = C_X + d_{RGB-D} \cdot \cos \theta \\ Y'_{RGB-D} = C_Y + d_{RGB-D} \cdot \sin \theta \end{cases} \tag{21}$$

When the coordinates of the RGB-D sensor with respect to the wall have been obtained, it is necessary to translate the coordinates to the origin of the UCS using the position of the Kinect (X_{CORNER}, Y_{CORNER}). It is also necessary to consider the side of the wall where the sensor is placed in order to select the sign of the X'_{RGB-D} and Y'_{RGB-D} coordinates. If the signs of the coordinates are positive, (22) shows how UCS coordinates are obtained.

$$\begin{cases} X_{UCS} = X_{CORNER} + X'_{RGB-D} \\ Y_{UCS} = Y_{CORNER} + Y'_{RGB-D} \end{cases} \tag{22}$$

IV. EXPERIMENTATION AND RESULTS

Twenty RGB-D sensors based on time-of-flight technology, Kinect v2, have been employed in these experiments. These devices deliver up to 2 MPx images (1920 x 1080) at 30Hz and 0.2 MPx *depth maps* with a resolution of 512 x 424 pixels. All these Kinect are connected to a web server where data are saved and processed. The horizontal field of view of the RGB-D sensor is 70°. This system generalizes our previous work that performed the same activity in a single room with a single RGB-D sensor. The system proposed is valid for a complete department or company where the position of each employee is useful to improve the efficiency of the business.

The experiments have been carried out in an office where twenty RGB-D cameras, Kinect v2, have been deployed (see Figure 5). There are eight different rooms with a central corridor with a total area of $80m^2$. In this corridor, four cameras have been deployed because of the range limitation of the sensor. Each camera is able to obtain skeletons in a 70° angle. The values of the coordinates of each skeleton have to be transformed into a universal coordination system (UCS). The central point of this UCS is situated on the left lower corner of the floor. The experiments have been developed considering the X and Y axis because all rooms are situated in the same floor.
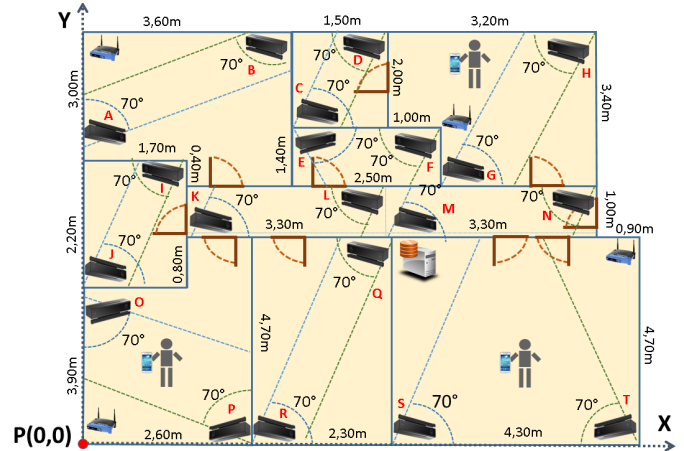

Figure 5. Scenario of the experiments

The Kinect sensors are placed in the corners using the X_{POS} and Y_{POS} displacements obtained by (8) and (9), which represent the distance between the Kinect and the corner. All these values, including the relative angle from the wall λ obtained by (16), are shown in Tables I and II. The distance between the corners, where the sensors are placed, and the origin of the UCS are also shown in Table I: X_{CORNER} and Y_{CORNER}. C_X and C_Y are also taken into account to obtain the displacement of the Kinect sensor in the UCS. These values represent the necessary distance to cover the maximum angle from the wall and are calculated according to (15), as seen previously. X_{UCS} and Y_{UCS} are calculated according to the expression shown in Table II where X'_{RGB-D} and Y'_{RGB-D} are obtained using (20) and (21). For example, the coordinates of a point obtained by the Kinect sensor E in the UCS are determined by (23).

TABLE I. TABLE OF PARAMETERS FOR KINECT PLACEMENT

Kinect RGB-D Camera	Corner to UCS X_{CORNER}	Corner to UCS Y_{CORNER}	Sensor to corner X_{POS}	Sensor to corner Y_{POS}	C_X	C_Y
A	0,00	6,10	0,21	0,14	0,07	0,10
B	3,60	9,10	-0,22	-0,13	0,06	0,11
C	3,60	7,10	0,13	0,21	0,06	0,11
D	5,10	9,10	-0,13	-0,21	0,06	0,11
E	3,60	7,10	0,13	-0,21	0,07	0,11
F	6,10	7,10	-0,13	-0,21	0,07	0,11
G	6,10	5,70	0,13	0,21	0,07	0,11
H	8,30	9,10	-0,14	-0,21	0,07	0,10
I	1,70	6,10	-0,13	-0,21	0,06	0,11
J	0,00	3,90	0,13	0,21	0,06	0,11
K	1,70	4,70	0,14	0,21	0,07	0,10
L	5,00	5,70	-0,14	-0,21	0,07	0,10
M	5,00	4,70	0,14	0,21	0,07	0,10
N	8,30	5,70	-0,14	-0,21	0,07	0,10
O	0,00	3,90	0,21	-0,14	0,07	0,10
P	2,60	0,00	-0,21	0,14	0,07	0,10
Q	4,90	4,70	-0,13	-0,21	0,07	0,11
R	2,60	0,00	0,13	0,21	0,07	0,11
S	4,90	0,00	0,14	0,21	0,07	0,10
T	9,20	0,00	-0,14	0,21	0,07	0,10

TABLE II. TABLE OF PARAMETERS FOR KINECT PLACEMENT

Kinect RGB-D Camera	L	λ	X_{UCS}	Y_{UCS}
A	3,00	1,37°	$X_{CORNER} + Y'_{RGB-D}$	$Y_{CORNER} + X'_{RGB-D}$
B	3,40	1,10°	$X_{CORNER} - Y'_{RGB-D}$	$Y_{CORNER} - X'_{RGB-D}$
C	1,50	2,63°	$X_{CORNER} + X'_{RGB-D}$	$Y_{CORNER} + Y'_{RGB-D}$
D	1,50	2,63°	$X_{CORNER} - X'_{RGB-D}$	$Y_{CORNER} - Y'_{RGB-D}$
E	2,50	1,61°	$X_{CORNER} + X'_{RGB-D}$	$Y_{CORNER} - Y'_{RGB-D}$
F	2,50	1,61°	$X_{CORNER} - X'_{RGB-D}$	$Y_{CORNER} - Y'_{RGB-D}$
G	2,20	1,82°	$X_{CORNER} + X'_{RGB-D}$	$Y_{CORNER} + Y'_{RGB-D}$
H	3,20	1,26°	$X_{CORNER} - X'_{RGB-D}$	$Y_{CORNER} - Y'_{RGB-D}$
I	1,70	2,33°	$X_{CORNER} - X'_{RGB-D}$	$Y_{CORNER} - Y'_{RGB-D}$
J	1,70	2,33°	$X_{CORNER} + X'_{RGB-D}$	$Y_{CORNER} + Y'_{RGB-D}$
K	3,30	1,23°	$X_{CORNER} + X'_{RGB-D}$	$Y_{CORNER} + Y'_{RGB-D}$
L	3,30	1,23°	$X_{CORNER} - X'_{RGB-D}$	$Y_{CORNER} - Y'_{RGB-D}$
M	3,30	1,23°	$X_{CORNER} + X'_{RGB-D}$	$Y_{CORNER} + Y'_{RGB-D}$
N	3,30	1,23°	$X_{CORNER} - X'_{RGB-D}$	$Y_{CORNER} - Y'_{RGB-D}$
O	3,90	1,04°	$X_{CORNER} + Y'_{RGB-D}$	$Y_{CORNER} - X'_{RGB-D}$
P	4,70	0,87°	$X_{CORNER} - Y'_{RGB-D}$	$Y_{CORNER} + X'_{RGB-D}$
Q	2,30	1,74°	$X_{CORNER} - X'_{RGB-D}$	$Y_{CORNER} - Y'_{RGB-D}$
R	2,30	1,74°	$X_{CORNER} + X'_{RGB-D}$	$Y_{CORNER} + Y'_{RGB-D}$
S	4,30	0,94°	$X_{CORNER} + X'_{RGB-D}$	$Y_{CORNER} + Y'_{RGB-D}$
T	4,30	0,94°	$X_{CORNER} - X'_{RGB-D}$	$Y_{CORNER} + Y'_{RGB-D}$

$$\begin{cases} X_{E,UCS} = 3,60 + X'_{E,RGB-D} \\ Y_{E,UCS} = 7,10 - Y'_{E,RGB-D} \end{cases} \quad (23)$$

where $X'_{E,RGB-D}$ and $Y'_{E,RGB-D}$ are obtained by (24).

$$\begin{cases} X'_{E,RGB-D} = 0,07 + d_{E,RGB-D} \cdot \cos\theta \\ Y'_{E,RGB-D} = 0,11 + d_{E,RGB-D} \cdot \sin\theta \end{cases} \quad (24)$$

$d_{E,RGB-D}$ and θ are calculated with (25) and (26) respectively.

$$d_{E,RGB-D} = \sqrt{Z^2_{E,RGB-D} + X^2_{E,RGB-D}} \quad (25)$$

$$\theta = 35 - 1,61 - \arcsin\left(\frac{X_{E,RGB-D}}{d_{E,RGB-D}}\right) \quad (26)$$

Finally, (27) shows how to obtain $X_{E,UCS}$ and $Y_{E,UCS}$ coordinates from the Kinect coordinates $X_{E,RGB-D}$ and $Y_{E,RGB-D}$.

$$\begin{cases} X_{E,UCS} = 3,67 + d_{E,RGB-D} \\ \quad \cdot \cos\left(33,39 - \arcsin\left(\frac{X_{E,RGB-D}}{d_{E,RGB-D}}\right)\right) \\ Y_{E,UCS} = 6,99 - d_{E,RGB-D} \\ \quad \cdot \sin\left(33,39 - \arcsin\left(\frac{X_{E,RGB-D}}{d_{E,RGB-D}}\right)\right) \end{cases} \quad (27)$$

The combination of WPS and RGB-D trajectories has been performed using the *Synchronized Euclidean distance* [15], as detailed in [2]. The developed experiments have shown an important advance in terms of indoor positioning. The system is able to locate more than 10 people with a success over 95% (see Figure 6) in a scenario with multiple rooms.
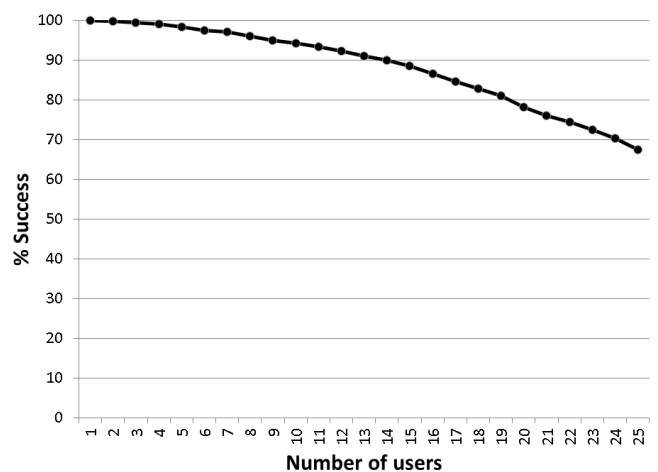

Figure 6. Results for a different number of users

V. CONCLUSIONS

This work presents an extended method for indoor positioning based on a previously developed algorithm, which worked exclusively with one room. This new method allows obtaining indoor positioning inside a complete floor or building. Twenty RGB-D sensors have been used to obtain the *depth maps* and, subsequently, the skeletons of users. The combination of wireless networks with skeletons is a simple and economical method to increase the performance of WPS in interiors. The generalization of the previous IPS allows obtaining the user positions in large areas where there are several users. The trajectories of users can be obtained by combining the two considered information sources: the WPS trajectories and the trajectories of the skeletons of the users in the *depth map*. Although the positioning of the wireless sensors in the complete scenario does not represent a real problem, special attention has been paid to the location of the depth cameras. The purpose of this has been to avoid blind areas, minimizing the total uncovered area. The work has also shown how coordinates obtained from the depth cameras at different rooms are transformed into a universal coordinates system (UCS). At this point, the previous technique can be applied to obtain

users positions and trajectories. The position of the sensors is followed by [16], where authors consider the use of this system to obtain the positions of the users in a museum, being this an approach to enrich the indoor users experience.

CONFLICTS OF INTEREST

The authors declare that there is no conflict of interest regarding the publication of this manuscript.

ACKNOWLEDGMENTS

REFERENCES

[1] G. Deak, K. Curran, and J. Condell, "A survey of active and passive indoor localisation systems," Computer Communications, vol. 35, no. 16, 2012, pp. 1939–1954.

[2] J. Duque Domingo, C. Cerrada, E. Valero, and J. Cerrada, "Indoor positioning system using depth maps and wireless networks," Journal of Sensors, vol. 2016, 2016.

[3] W. Liu, Y. Chen, Y. Xiong, L. Sun, and H. Zhu, "Optimization of sampling cell size for fingerprint positioning," International Journal of Distributed Sensor Networks, vol. 2014, 2014.

[4] S. He and S.-H. G. Chan, "Wi-fi fingerprint-based indoor positioning: Recent advances and comparisons," IEEE Communications Surveys & Tutorials, vol. 18, no. 1, 2016, pp. 466–490.

[5] G. Ye, Y. Liu, Y. Deng, N. Hasler, X. Ji, Q. Dai, and C. Theobalt, "Free-viewpoint video of human actors using multiple handheld kinects," Cybernetics, IEEE Transactions on, vol. 43, no. 5, 2013, pp. 1370–1382.

[6] H. Takizawa, S. Yamaguchi, M. Aoyagi, N. Ezaki, and S. Mizuno, "Kinect cane: object recognition aids for the visually impaired," in Human System Interaction (HSI), 2013 The 6th International Conference on. IEEE, 2013, pp. 473–478.

[7] Y. Nakano, K. Izutsu, K. Tajitsu, K. Kai, and T. Tatsumi, "Kinect positioning system (kps) and its potential applications," in International Conference on Indoor Positioning and Indoor Navigation, vol. 13, 2012, p. 15th.

[8] C. K. Schindhelm, "Evaluating slam approaches for microsoft kinect," in Proc. 2011 The Eighth International Conference on Wireless and Mobile Communications (ICWMC 2012), Venice, 2012, pp. 402–407.

[9] P. Mirowski, R. Palaniappan, and T. K. Ho, "Depth camera slam on a low-cost wifi mapping robot," in Technologies for Practical Robot Applications (TePRA), 2012 IEEE International Conference on. IEEE, 2012, pp. 1–6.

[10] J. Machaj and P. Brida, "Impact of optimization algorithms on hybrid indoor positioning based on gsm and wi-fi signals," Concurrency and Computation: Practice and Experience, 2016.

[11] A. Papapostolou and H. Chaouchi, "Integrating rfid and wlan for indoor positioning and ip movement detection," Wireless Networks, vol. 18, no. 7, 2012, pp. 861–879.

[12] J. Biswas and M. Veloso, "Multi-sensor mobile robot localization for diverse environments," in RoboCup 2013: Robot World Cup XVII. Springer, 2014, pp. 468–479.

[13] J. Shotton, T. Sharp, A. Kipman, A. Fitzgibbon, M. Finocchio, A. Blake, M. Cook, and R. Moore, "Real-time human pose recognition in parts from single depth images," Communications of the ACM, vol. 56, no. 1, 2013, pp. 116–124.

[14] A. Barmpoutis, "Tensor body: Real-time reconstruction of the human body and avatar synthesis from rgb-d," Cybernetics, IEEE Transactions on, vol. 43, no. 5, 2013, pp. 1347–1356.

[15] C. T. Lawson, S. Ravi, and J.-H. Hwang, "Compression and mining of gps trace data: New techniques and applications," Technical Report. Region II University Transportation Research Center, Tech. Rep., 2011.

[16] J. Duque-Domingo, P. J. Herrera, E. Valero, and C. Cerrada, "Deciphering egyptian hieroglyphs: Towards a new strategy for navigation in museums," Sensors, vol. 17, no. 3, 2017, p. 589.